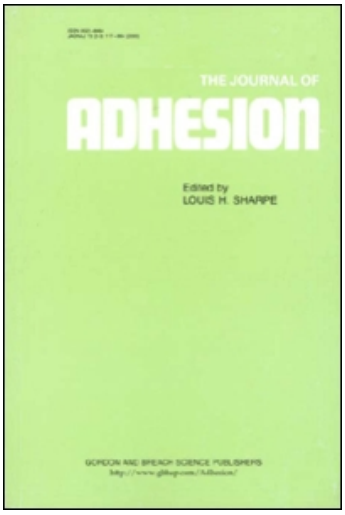

The Journal of Adhesion
Publication details, including instructions for authors and subscription information:
http://www.informaworld.com/smpp/title~content=t713453635

On the Effects of Processing Conditions and Interphase of Modification on the Fiber/Matrix Load Transfer in Single Fiber Polypropylene Composites

F. Hoecker[a]; J. Karger-Kocsis[a]
[a] Institute for Composite Materials Ltd., University of Kaiserslautern, Kaiserslautern, Germany

To cite this Article Hoecker, F. and Karger-Kocsis, J.(1995) 'On the Effects of Processing Conditions and Interphase of Modification on the Fiber/Matrix Load Transfer in Single Fiber Polypropylene Composites', The Journal of Adhesion, 52: 1, 81 — 100
To link to this Article: DOI: 10.1080/00218469508015187
URL: http://dx.doi.org/10.1080/00218469508015187

J. Adhesion, 1995, Vol. 52, pp. 81–100
Reprints available directly from the publisher
Photocopying permitted by license only

On the Effects of Processing Conditions and Interphase of Modification on the Fiber/Matrix Load Transfer in Single Fiber Polypropylene Composites*

F. HOECKER and J. KARGER-KOCSIS

Institute for Composite Materials Ltd., University of Kaiserslautern, P.O. Box 3049, D-67653 Kaiserslautern, Germany

(Received March 8, 1994; in final form May 17, 1994)

The scope of this study was the investigation of the effects of both processing conditions (in terms of thermo-mechanical history) and interphase modification (fiber sizing and/or matrix coupling) on the interfacial shear strength (τ_i) of fiber reinforced isotactic polypropylene (iPP). Fiber/matrix load transfer efficiency was investigated by modified single fiber pullout and microdroplet pulloff test methods, respectively. It was established that τ_i of the neat microcomposite (unsized fiber/uncoupled matrix) is improved by quenching of the samples rather than by various spherulitic or transcrystalline supermolecular structures set under isothermal crystallization conditions. Enhanced interfacial shear strength for the quenched samples was attributed to a better wetting behaviour and a fine dispersion of the amorphous PP (aPP) fraction formed. An adhesion model was proposed based on which optimum τ_i is linked to both matrix strength and its wetting behaviour. It was demonstrated that the results from pullout and pulloff tests correlate very well with each other for the particular glass fiber/iPP model composite systems studied. It was shown further that matrix modification (coupling) or fiber sizing enhances τ_i practically to the same level, whereas a combination of matrix coupling and fiber sizing yields an even higher interfacial shear strength (synergistic effect).

KEY WORDS glass fiber; polypropylene; composites; adhesion; morphology; interfacial shear strength; crystallization; supermolecular structures; single fiber pullout test; wetting; microdroplet pulloff test.

INTRODUCTION

The mechanical property profile of fibrous composites is mainly determined by the composition, arrangement, and inherent properties of their constituents, *i.e.*, matrix and reinforcement, such as fiber volume fraction, fiber aspect ratio, fiber orientation, strengths, moduli, and physical properties of the matrix and fibers, respectively. In addition to those factors, the nature and quality of the adhesion between fibers and matrix, *i.e.*, the characteristics of the interphase, are widely recognized to affect the mechanical performance of composites. This scenario becomes even more complex in semicrystalline thermoplastic materials where changes in the matrix morphology arise during processing. So, in particular, processing-induced microstructural changes or

* One of A Collection of papers honoring Lawrence T. Drzal, the recipient in February 1994 of *The Adhesion Society Award for Excellence in Adhesion Science, Sponsored by 3M.*

supermolecular formations adjacent to the fibers are to be taken into account, also. These features may affect the fiber/matrix adhesion and can thus be treated as additional interphase parameters.

During the past many years several studies have been performed in the fields of interface morphology (single fiber model composites) and structure/property–relationships (real composites) for various fiber/matrix combinations, but the link between interface morphology and the mechanical properties of the interphase has remained unsolved. It is not clear so far whether different morphological arrangements, induced by the processing of thermoplastic composites, substantially affect the interfacial shear strength (τ_i) and the related failure mechanisms or not. For example, reports on the effects of transcrystalline superstructures (as first described for high polymers by Jenckel *et al.*,[1] in 1952 and demonstrated by zone solidification in a temperature gradient by Lovinger *et al.*[2]) developed around the reinforcing fibers are controversial. A decrease (GF/PP[3] and CF/J-polymer[4]), no clear influence (PE/PE[5]), and an increase in the (micromechanically-gained) interfacial shear strength (GF/PP,[6] CF/PEEK,[7] and CF/PPS[7]) were found. Furthermore, recent publications of Wagner *et al.*,[8] Tregub *et al.*,[9] and Meretz *et al.*,[10] reveal not unambiguously that mechanical property profile and failure mechanism of composites are considerably influenced by both morpology and crystallinity of matrix and interphase. Therefore, as far as semicrystalline thermoplastic matrix materials are taken into account, Drzal's interphase design strategy [11] developed for optimum processing and performance has to be completed by adequate processing conditions.

"Micromechanical" or "model test methods," as reviewed and developed by Drzal,[12,13] are conducted on single fiber specimens in order to realize an "isolated and quantitative" determination of the fiber/matrix interfacial shear strength and the change of this parameter on definite interface variations.

In this study, the classical single fiber pullout test was modified in order to investigate the effects of matrix and, thus, interphase morphology on the interfacial shear strength, separately. This pullout technique was first described by Kobayashi *et al.*,[7] and enables the "simulation" of thermal or thermo-mechanical composite processing (thermal history, melt shearing, etc.). Furthermore, this adapted technique allows one to modify the interface morphology and matrix microstructure under controlled conditions, to monitor the crystallization *in situ* by means of transmitted light microscopy, and to determine the interfacial shear strength and failure mechanisms on "consolidated" specimens. In addition to the aforementioned testing method the microdroplet pulloff test, using straight microvices, was employed. It was aimed at comparing the interfacial shear strength values derived from modified pullout and microdroplet pulloff tests.

EXPERIMENTAL

Materials

The model matrix material used in this study was isotactic polypropylene ("neat" and "coupled" iPP). iPP was chosen as representative of semicrystalline thermoplastics, mainly due to its widespread use and polymorphism[14–16] dependent on the crystalli-

zation conditions. The glass fibers (GF, ∅ 14 μm) were unsized and commercially sized for PP, respectively. Both of the above materials were available in the form of GF/PP commingled yarns (50 wt% GF), provided by an industrial partner. The melt flow index of the general purpose multifilament iPP grade was 20 dg/min (230°C, 2.16 kg). The influence of the matrix/interphase morphology was studied by the modified pullout test using unmodified iPP and unsized GF, whereas for those of coupling (matrix modification) and fiber sizing the microdroplet pulloff technique served. Coupling was achieved by adding to the above iPP 5 wt% of a maleic-anhydride grafted iPP. Furthermore, the effect of GF with an aqueous sizing was studied, as well.

Sample Preparation

Microcomposites for the modified pullout test were prepared by placing a thin strip of iPP film on a microscope cover glass, and one single GF was positioned perpendicular to the film before covering this "package" with another glass sheet. GF/iPP samples were produced by heating the package up to 200°C and holding there for a few minutes in order to avoid microstructural memory effects in the matrix.[17] Samples were prepared either in a Heraeus thermostatic chamber followed by quenching in iced water or, alternatively, in a hot stage of a Leitz transmitted light microscope during isothermal crystallization conditions. The latter case was carried out either in quiescent melt or after melt shearing realized by pulling the fiber in the supercooled polymer melt as the isothermal crystallization temperature (T_c) was reached. Figure 1 shows the experimental set-up of the modified pullout test and a characteristic sample after removing both the upper and the lower glass cover sheets.

Samples for the microdroplet pulloff tests were prepared by hanging up microtomed PP chips onto the GF. Droplets were formed after heating these specimens in a thermostatic chamber under the aforementioned conditions. Consolidation of the single fiber microcomposites was always realized by air-cooling. Figure 2 displays the experimental set-up and a GF/iPP microcomposite tested by the microdroplet pulloff technique.

Variation of the Matrix Microstructure

All the different matrix microstructures set in GF/iPP within the frame of this study were achieved solely by altering the crystallization conditions. The apparent degrees of crystallinity, X_c, were established by differential scanning calorimetry (DSC) measurements using a Mettler TA 4000 thermoanalytical system supposing that the melting enthalpy of the fully-crystalline iPP ($\Delta H_{c,100\%,iPP}$) is 190 J/g. Crystallizing the GF/iPP sample isothermally at $T_c = 140°C$ (Figure 3a; $X_c = 52.5\%$; $\varnothing_{spher} = 200...300$ μm) and $T_c = 135°C$ ($X_c = 46.4\%$; $\varnothing_{spher} = 120...200$ μm) resulted in a coarse α-spherulitic matrix structure,[18] whereas quenching the specimens in iced water led to a finely-dispersed morphology in which supermolecular structures could hardly be resolved (Figure 3b; $X_c = 42.5\%$). It is obvious from Figure 3 that variations in the crystallization and/or cooling conditions alone do not promote nucleation by the GF surface. The microstructure of the pure PP-matrix is not influenced by the GF present; no transcrystallization occured. Nevertheless, the cooling rates and crystallization tem-

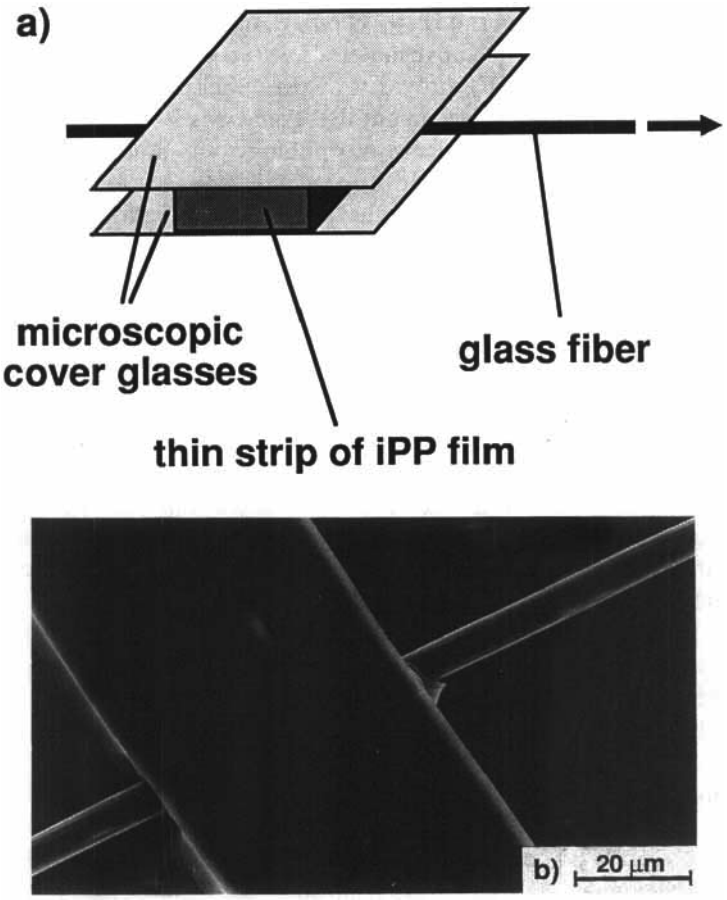

FIGURE 1 Modified single fiber pullout testing technique: a) experimental set-up, b) SEM of a single fiber pullout specimen.

peratures affected the matrix morphology substantially: Higher T_c originated less but, therefore, larger and structurally more perfect spherulites, and increasing cooling rates reduced the degree of crystallinity.

Transcrystalline-like superstructures in GF/iPP could only be achieved by melt shearing, *i.e.*, by pulling the GF partially through the isothermally crystallizing iPP. Melt shearing is supposed to generate a layer of well-oriented (with respect to the fiber axis) polymer chains along the fiber surface.[15,16] This layer exhibits a strong nucleation ability for homogeneous crystallization. Therefore, this phenomenon should henceforth be called row-nucleated cylindritic or columnar crystallization rather than transcrystallization (the latter is a special type of heterogenous crystallization).[17,19] Figure 4b shows schematically that "transcrystallization" appears when the spherulite growth is restricted to one direction, *i.e.*, perpendicular to the substrate, here the fiber surface. Furthermore, it is obvious from Figure 4 that this supermolecular structure becomes more "uniform" with increasing nucleation density on the substrate surface.

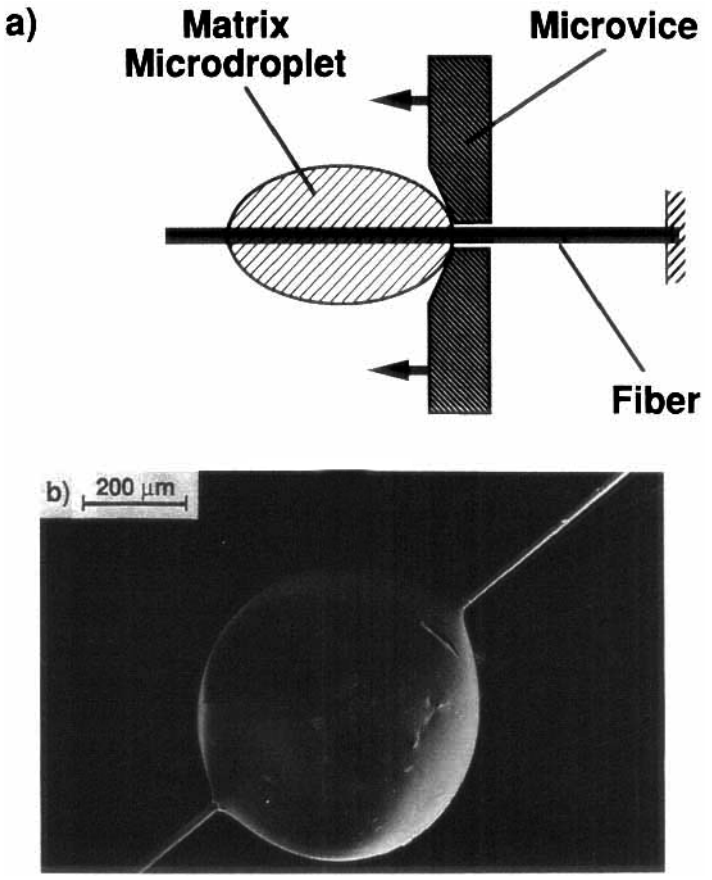

FIGURE 2 Microdroplet pulloff test: a) experimental set-up, b) SEM of a tested specimen.

Nucleation density itself is reported to depend, however, on a variety of possible fiber/matrix interactions or mismatches in the crystal unit cells.[20,21] As evidenced in Figure 4a, transcrystallinity is strictly related to spherulitic crystallization.[15,22] In particular, the growth rates and lamellar orientations (as assessed by means of light birefringence[1,18,23]) of three-dimensionally growing spherulites and correlating cylindrites are similar. This correspondence can further be proved by the texture of the isothermally crystallized ($T_c = 140°C$) GF/iPP specimen after melt shearing (Figure 4a). It is unambiguously demonstrated that spherulitic and cylindritic crystallization are of one and the same origin. Growth rates as well as lamellar orientations are identical for both features. In addition, a large spherulite develops at the right end of the pulled fiber where its growth is not restricted due to a high nucleation density. It is noteworthy that there was no significant difference in the degree of crystallinity between the samples with spherulitic and cylindritic matrix morphologies.

Depending on the melt shearing temperature and temperature of isothermal crystallization, α-cylindrites (monoclinic lattice, $T_c = 140°C$, lower growth rates, see

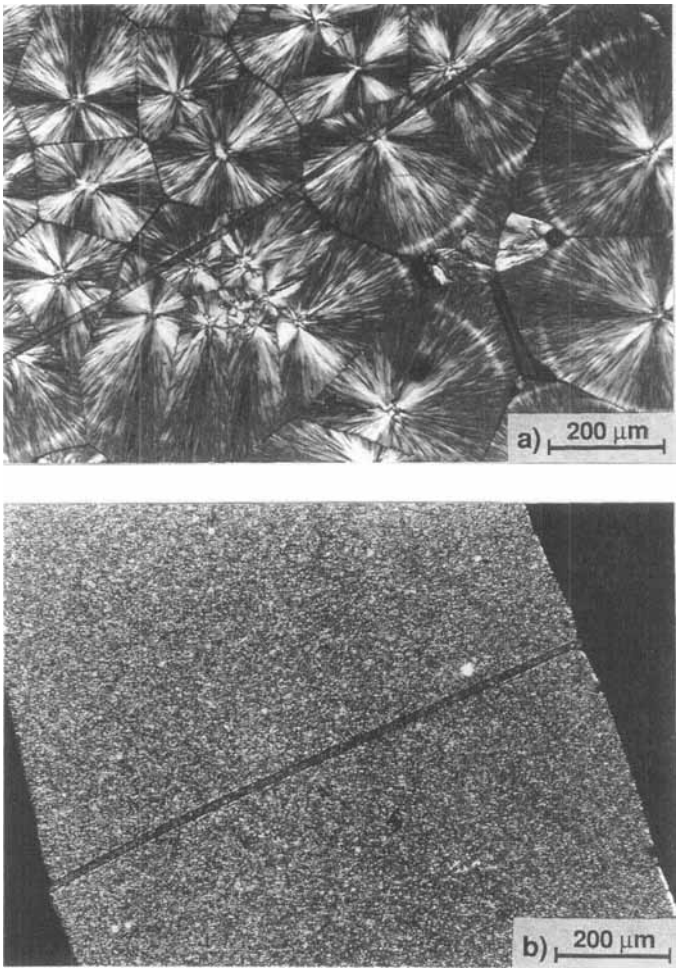

FIGURE 3 a) Coarse α-spherulitic superstructure in GF/iPP (T_c = 140 °C) and b) Finely dispersed morphology in a quenched GF/iPP sample.

Figure 5a) or β-cylindrites (hexagonal lattice, $T_c = 135$°C, higher growth rates, see Figure 5b) may form according to the appearance of corresponding spherulites in the bulk matrix.[2,15,24]

Variation of the Interphase Chemistry

Figure 6 compares a section of the FT-IR spectrum taken from a hot pressed film of the coupled PP matrix with that of a commercially-available, maleicanhydride (MA)-modified iPP homopolymer (Polybond 3150, British Petroleum) having an MFI value of *ca.* 50 dg/min (230°C, 2.16 kg). The IR-spectra were taken by a Nicolet 510 M spectrophotometer in transmittance mode using 256 scans at a resolution of 0.8 cm^{-1}. Surprisingly, the CO absorption of the MA at about 1780 cm^{-1} is not well resolved in

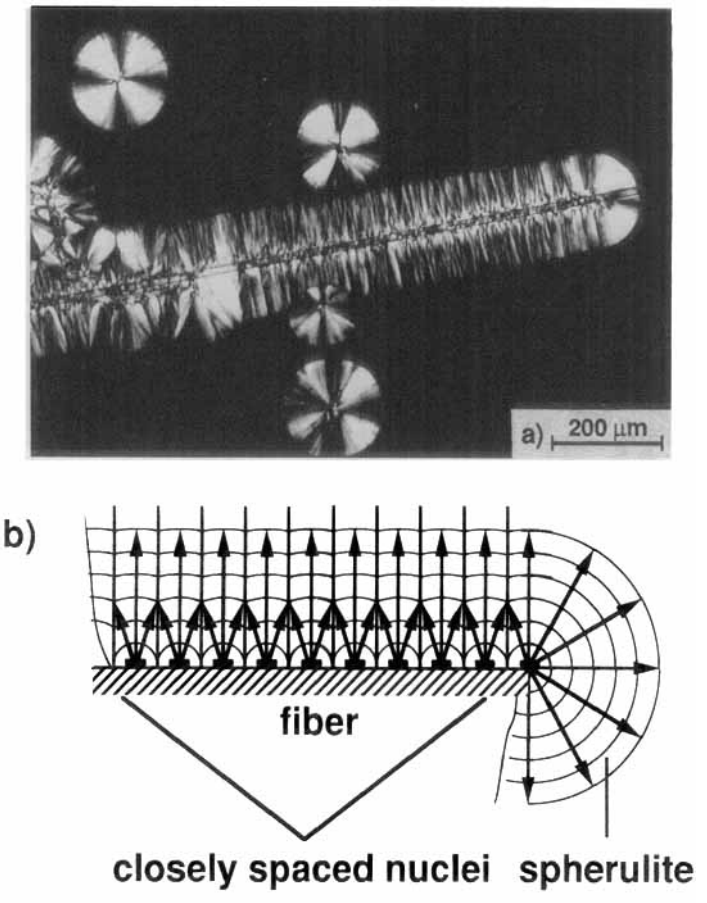

FIGURE 4 Crystallization features as a function of nucleation density: a) cylindritic crystallization after melt shearing ($T_c = 140$°C) and b) schematic representation of a.

both samples. The absorption bands in the wavenumber range of 700 to 1450 cm^{-1} can be assigned according to the work of Painter *et al.*[25]

Testing and Data Reduction

Modified single fiber pullout and/or microdroplet pulloff tests were performed on the specimens (prepared as described before) using two specially-designed and tailor-made micro-tensile testing machines equipped with highly precise Hottinger-Baldwin load (Q11, full range: 1N) and displacement (W10, full range: 10 mm) transducers. These devices allowed the tests to be monitored visually by transmitted and stereo light microscopy, respectively. Pullout speed (0.5 mm/min) and fiber free lengths (7...8 mm) were kept constant in order to achieve similar conditions in terms of stored elastic energy (mainly in the fiber free length) for interface failure initiation and propagation. The embedded fiber lengths varied in a range from 500 to 1500 µm (modified pullout

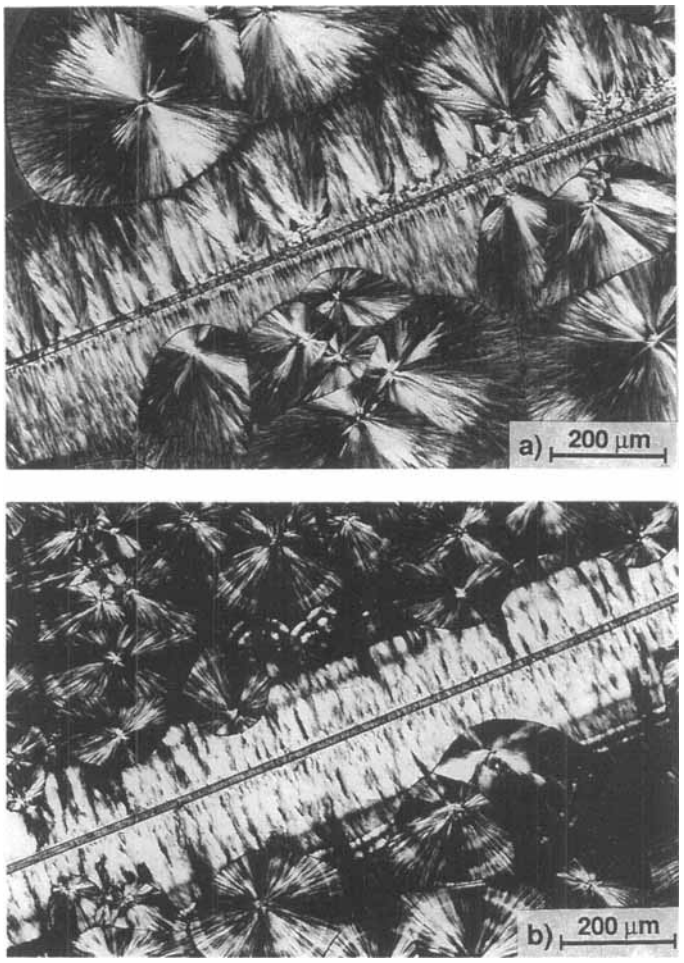

FIGURE 5 a) α-cylindrite after melt shearing ($T_c = 140°C$) and b) β-cylindrite after melt shearing ($T_c = 135°C$).

test) and 100 to 500 µm (microdroplet pulloff test), according to the specific sample preparation techniques. Load-displacement curves were monitored on an x–y plotter. Interfacial failure occured when the applied force reached the maximum value, F_{max}, and dropped subsequently.

As iPP is a ductile material, uniform shear yielding of the interface is assumed, *i.e.*, the shear-stress-criterion is used for data reduction. The apparent interfacial shear strength (τ_i) value was, therefore, directly calculated by:

$$\tau_i = \frac{F_{max}}{\pi DL}$$

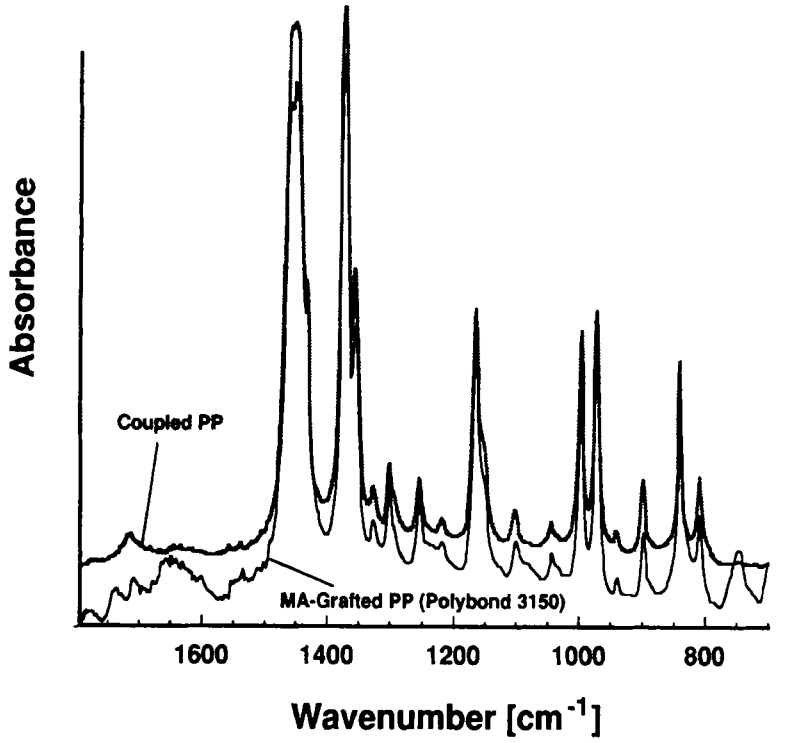

FIGURE 6 Comparison of the FT-IR spectrum of the coupled PP with that of a commercially-available MA-grafted iPP (Polybond 3150, British Petroleum).

where F_{max} is the maximum tensile load, D and L are fiber diameter and embedded fiber length, respectively. Alternatively, τ_i may be estimated from the slope of the graphs showing F vs. L, whereby straight lines are related to shear-stress-controlled interphase failure.

The validity of the shear-stress-criterion could further be confirmed by microscopic observations *in situ* during the tests. Interfacial failure occured abruptly along the whole embedded fiber length rather than by stepwise debonding (propagation-type debonding). The latter was proposed for brittle interphases and initiated the use of energy-related failure criteria.[26]

RESULTS AND DISCUSSION

Processing Conditions

Results The interfacial strength values, τ_i, obtained by the modified pullout testing technique on GF/iPP-samples of varying matrix microstructure/morphology are summarized in Figure 7 and Table I. Both mean values of at least 10 samples for each

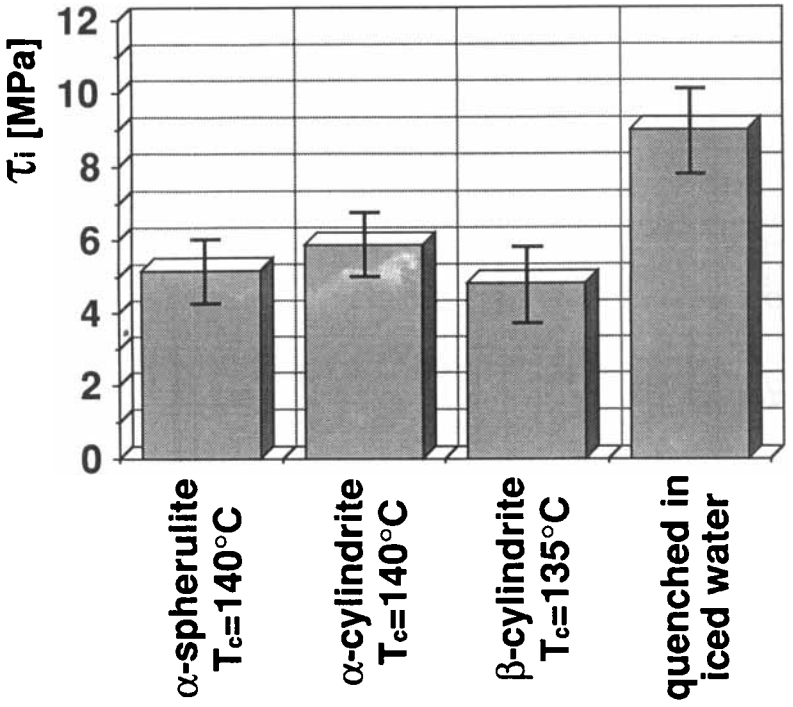

FIGURE 7 Interfacial shear strength as a function of matrix microstructure for GF/iPP (modified pullout test).

modification and the related standard deviations are indicated. In general, it is conspicuous that even the highest τ_i-values, *i.e.*, ~ 9 MPa for the quenched specimens, are far below the shear yield strength of the neat iPP (~30 MPa). This indicates clearly an insufficient level of adhesion between GF and iPP. Furthermore, changes in the supermolecular structures around the GF (spherulite/cylindrite) seem not to enhance

TABLE I
Interfacial shear strength values for the modified pullout test

Material	Thermal History	Supermolecular Structure	τ_i(mean) [MPa]	τ_i(st. dev.) [MPa]
GF/iPP	quenched	finely dispersed	9,0	1,9
GF/iPP	quenched + annealed	finely dispersed	5,6	1,6
GF/iPP	$T_c = 140°C$	α-spherulitic	5,1	1,4
GF/iPP	$T_c = 140°C$	α-cylindritic	5,8	1,6
GF/iPP	$T_c = 135°C$	β-cylindritic	4,8	1,7
GF/aPP	quenched	—	0,6	0,2
GF/aPP	$T_h = 140°C$		0,4	0,1
CF/iPP	quenched	finely dispersed	5,1	1,9
CF/iPP	$T_c = 140°C$	α-spherulitic	5,3	1,8
CF/iPP	$T_c = 140°C$	α-cylindritic	5,2	1,3

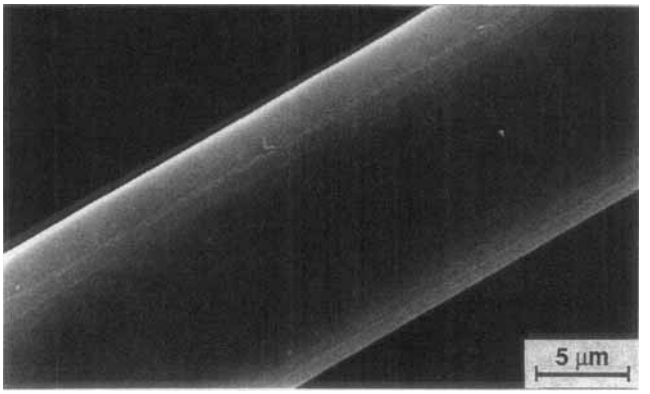

FIGURE 8 Adhesive-type interface failure in GF/iPP (modified pull-out test).

the adhesion at all ($\tau_i \sim 4...6$ MPa); only rapid cooling proved to be beneficial. The latter effect has also been observed on UHMWPE/LLDPE specimens by Rolel *et al.*,[5] recently. In general, the typical failure mechanism is poor adhesive-type for all the modifications studied. Therefore, the pulled-out GF-regions are bare, no matrix residues can be resolved by SEM (see Figure 8). The shear strength values obtained in this part of the present work (4.8–9.0 MPa) fit well in the τ_i-range (4.5–8.4 MPa) published in the recent literature for GF/iPP and based on various micromechanical testing methods.[6,26,27]

Discussion

Matrix/Interphase Morphological Effects. As explained earlier in this paper, α-transcrystalline zones or, more precisely, α-cylindrites and α-spherulites, are of the same α-spherulitic nature. Therefore, the adhesion of GF to iPP should not be influenced effectively by the formation of different supermolecular structures around the fibers. However, there are certainly differences in nucleation density on and near the glass fiber surface. *A priori*, "transcrystallinity" might be estimated to promote adhesive friction between matrix and reinforcing fiber by increased radial compressive stresses due to the fiber being subjected to inner spherulitic pressure.[28] In fact, the fiber is surrounded by closely-spaced spherulitic sites, but effects on the interface mechanical performance could not be resolved by the modified pullout testing technique performed.

Furthermore, for the β-cylindritic structure, it could be proved, as published by Varga and Karger-Kocsis,[17,19] that these structures consist of two layers. In the vicinity of the pulled glass fiber, α-row-nuclei of higher thermal stability (since they were grown at higher temperatures) develop due to melt shearing. These α-row-nuclei exhibit a very high selective β nucleation ability at $T_c = 135$°C which results in the growth of β-cylindrites. Since the growth rate of the β-form is higher than the α one at 135°C, the resulting β-cylindrite looks like a β-transcrystalline layer. The occluded α-phase is difficult to resolve optically, but its presence was evidenced by selectively re-melting the (thermally less stable, since grown at lower temperatures) β-cylindrite at

$T = 155°C$ (see Figure 9a). The scheme on this phenomenon, presented in Figure 9b, confirms that the resulting superstructure is cylindritic rather than transcrystalline due to a homogeneous crystallization featuring an α-β bifurcation. Figure 10a shows a β-cylindritic structure surrounded by α-spherulites after etching by chromic acid (composition: $K_2Cr_2O_7$: H_2O:H_2SO_4 = 4.4:7.1:88.5 wt%, temperature 70°C, immersion time: 10 min). It is obvious that the β-modification is not only thermally but also chemically less stable than the α-one. This etching technique can be used, therefore, to demonstrate the presence of an α-layer beneath the fiber bed within a β-cylindritic supermolecular formation (Figure 10b).

Thus, again an α-spherulitic structure is relevant for the adhesion to the GF, even when a β-cylindrite formed around the GF. Hence, the interfacial shear strength must remain at the same level, which has been proved, indeed.

Matrix Crystallinity Effects. There are, in principle, two possible effects that may explain the improved adhesion observed between GF and iPP when the samples were

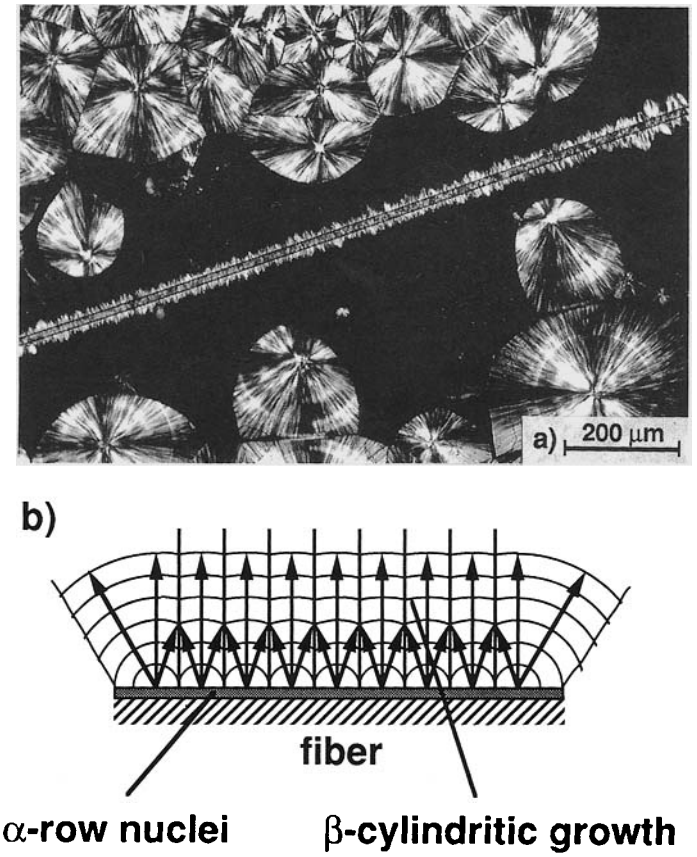

FIGURE 9 Nature of β-cylindrites: a) after selective remelting ($T = 155$ °C) and b) schematic representation of the α-β bifurcation and formation of β-cylindrites.

quenched: a) higher interfacial strength due to matrix thermal shrinkage and thus increased interfacial friction at failure initiation and during pullout and b) enhanced adhesion due to better wetting of the enlarged (lower degree of crystallinity) and more homogeneously dispersed amorphous PP (aPP) phase.

Referring to the thermal shrinkage, several authors, *e.g.*, Biro,[29] developed theoretical models in order to estimate frictional effects by considering the contribution of residual stresses to the "overall" adhesion between the matrix and the fiber. Although these models were originally worked out for thermoset matrix composites (given ΔT: curing temperature–room temperature), attempts have been made to modify them for thermoplastic matrix composites as well, *e.g.*, by DiLandro.[30] In spite of the fact that terms related to effective temperature differences, material viscosities, and morphological effects are very uncertain, some of these models (*e.g.*, Jang[31]) estimate τ_i quite well.

Since all the cited mechanical models are based on diferences in thermal expansion between fibers and matrices, tests with polyacrylonitrile (PAN)–based high-tenacity carbon fibers (CF, $\varnothing$ 7 μm) without fiber surface coating were also conducted. Samples were prepared and tested under the same conditions as described before. The interfacial

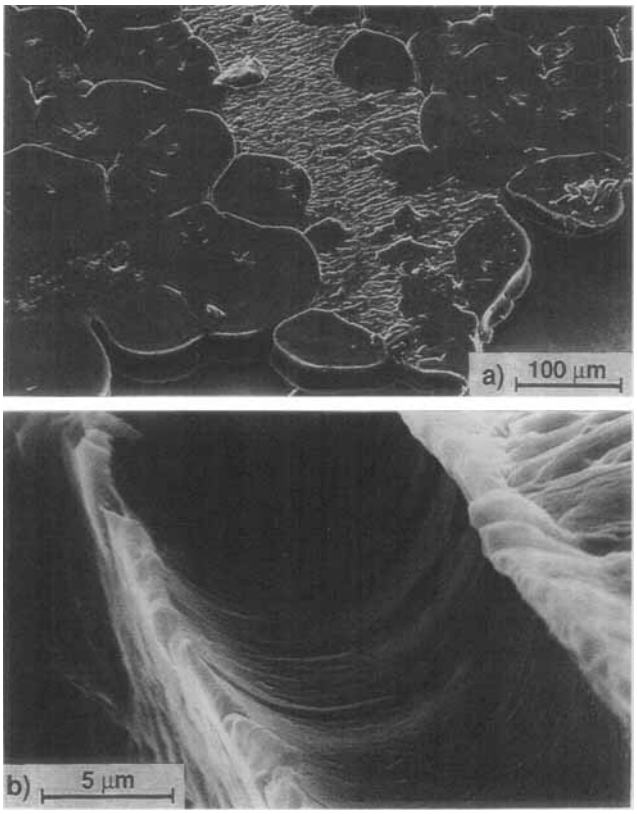

FIGURE 10 β-cylindritic structure (a) and α-layer in a β-cylindritic fiber bed (b) after etching by chromic acid.

shear strength was not expected to increase in CF/iPP due to enlarged compressive residual stresses since $\alpha_{th,rad}$ (CF) = $\alpha_{th,rad}$(GF). This was found, indeed (see Table I). The results are compared with those gained by GF/iPP specimens in Figure 11.

Again, it is striking that both combinations GF/iPP and CF/iPP exhibit a poor level of adhesion and an almost constant shear strength level. For CF/iPP, even quenching the sample in iced water had no beneficial effect. The interfacial shear strength in CF/iPP was not influenced by either the matrix morphology or by the cooling rate. Particularly for the quenched modifications, τ_i exhibits even higher values for GF/iPP than for CF/iPP. Besides that, no significant deviations in the level of dynamic interfacial friction was observed in the load-displacement curves registered. These facts indicate unambiguously that variations in the contribution (with respect to the "overall" adhesion) of mechanical friction due to different fiber thermal/residual clamping stresses are definitely not dominating parameters for the fiber/matrix adhesion in the GF/iPP used. Hence, we suppose that the increase of the shear strength is mainly due to the features and the location of the amorphous PP phase. The improvement of the interfacial shear strength for the quenched specimens is mainly attributed to both the enlarged amorphous fraction of the matrix (lower degree of crystallinity, X_c) and its fine dispersion (see Figure 3b). This texture leads to improved surface wetting and enhanced adhesion. The improved adhesion is thus related to the sticking nature of atactic PP (aPP), especially in the melt phase (therefore, aPP is the main component of several hot melt adhesives).

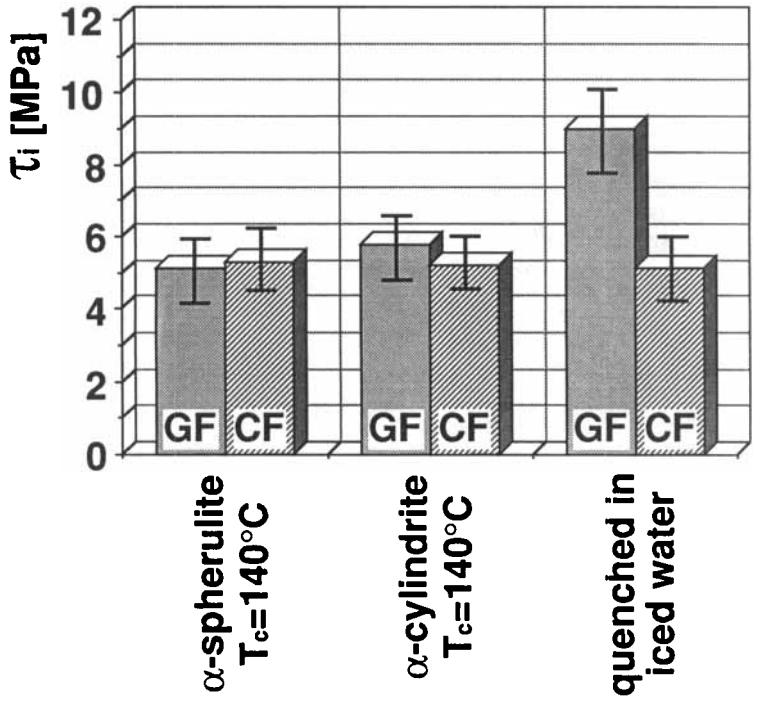

FIGURE 11 Comparison of interfacial shear strength for GF/iPP and CF/iPP (modified pullout test).

In order to check this hypothesis, complementary pullout tests on GF/aPP samples either isothermally held at 140°C or quenched in iced water were performed and compared with tests on GF/iPP specimens identically crystallized at 140°C and resulting in the formation of α-spherulites (see Table I).

It is obvious that the GF/aPP specimens exhibit very low interfacial shear strength and that there is no dependence on the cooling conditions to be detected. It should be noted here that τ_i agrees quite well with the yield strength of the aPP fraction used (~ 1 MPa).

Furthermore, SEM-fractographs on the failed GF/aPP interface sites (see Figure 12) show that, contrary to the adhesive-type interfacial failure of GF/iPP (see Figure 8), cohesive matrix failure occured that clearly indicates a) good wetting and b) insufficient matrix shear strength.

The superior wetting properties of aPP with respect to the glass fiber (GF) could be proved by measuring the apparent contact angles of iPP and aPP on a glass plate (GP) whose surface tension was determined to be ~ 25 mN/m following the Zisman method.[32] Samples were melted up to 200°C, in accordance with the preparation of the pullout specimens, then isothermally crystallized or held (140°C, 30 min) in a hot stage and subsequently measured at room temperature using a Ramé-Hart contact angle telegoniometer. The contact angle of iPP/GP was 55° whereas the aPP/GP sample exhibited a lower one of 35° which reveals better wetting of the glass plate by aPP. In addition, the iPP droplets were, in contrast to the aPP ones, fully debonded from the glass plate after cooling down to ambient temperature. This "de-wetting" phenomenon was attributed to different volume change mechanisms in iPP and aPP during sample consolidation (see Figure 13). Volume reduction by crystallization, superimposed on the cooling-induced thermal shrinkage, creates high shear forces at the iPP/GP interface which results in easy detaching from the GF surface.

On the basis of both wetting properties and material strengths an optimum in terms of adhesion and, consequently, load transfer capability (as estimated by the interfacial shear strength τ_i) can be provided by a proper "mixture" of iPP and aPP. In this case all the pre-requisites for good adhesion are met: a) good wetting behaviour (by the

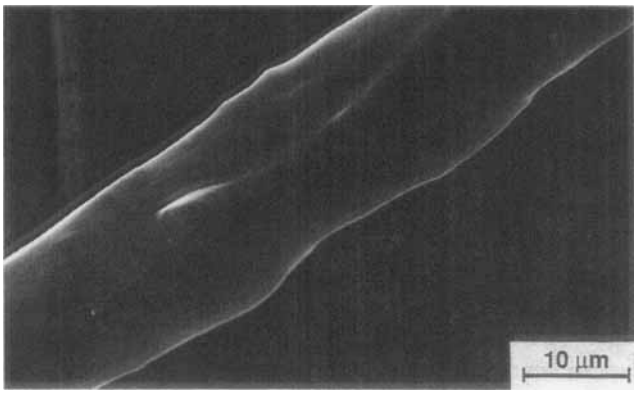

FIGURE 12 Cohesive matrix failure in GF/aPP (modified pullout test).

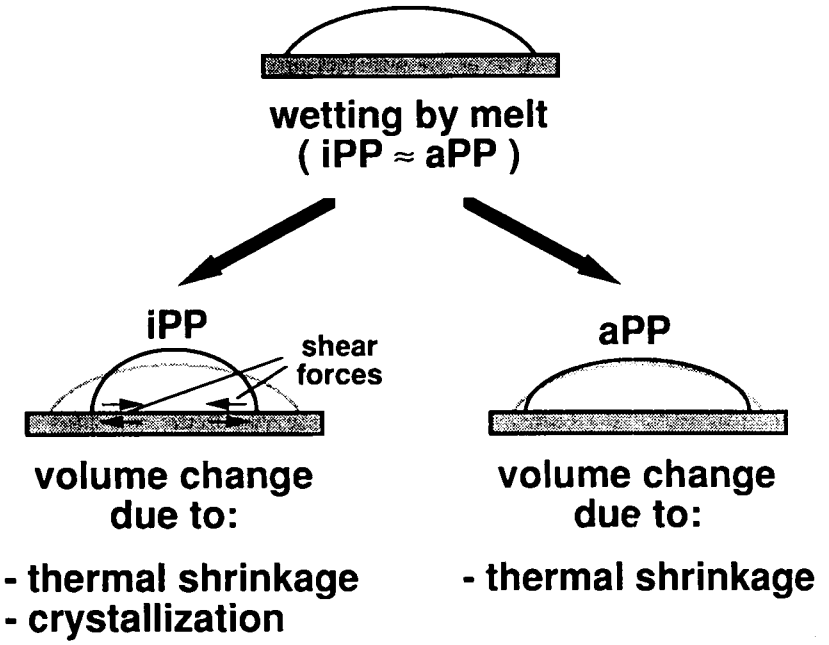

FIGURE 13 De-wetting mechanism in GF/iPP due to cooling and crystallization.

amorphous PP phase) and b) sufficient material strength (by the crystalline PP phase). Considering the matrix morphology and the degree of crystallinity of isothermally crystallized and quenched GF/iPP specimens, the "covered surface" (by the amorphous fraction) of the GF is much smaller in a coarse spherulitic structure where the amorphous phase is located between the lamellae and at the spherulite boundaries. It is obvious in Figure 14 that the geometrical probability of such aPP-enriched boundaries present along the fiber surface is much lower than in a quenched sample of fine texture. In the latter case, the amorphous phase has not been "ejected" during crystallization and, in addition, due to the rapid cooling, its fraction is also increased. So, in the quenched samples good wetting is maintained by a large amorphous PP phase and a finely-dispersed structure. On the other hand, the required high matrix strength is supplied by a "tight-mesh network structure" in which crystalline blocks are held together by tie molecules. The proposed adhesion model for GF/iPP suggests some kind of interpenetrating network built up by an amorphous and a crystalline PP phase. It should be noted here that an optimum in the wetting and strength performance can probably be obtained by using random PP copolymers.

This adhesion model proposed in our earlier publication[33] was confirmed by the fact that quenched and subsequently-annealed (140°C, 30 min) GF/iPP samples led to τ_i values similar to the isothermally-crystallized ones (see Table I). This was related to the dewetting mechanism depicted in Figure 13 caused by a post-crystallization process. Furthermore, recent studies by Ye *et al.*,[34] on mesostructural aspects of interlaminar fracture toughness in GF/PP composites, with special emphasis on the matrix crystallinity, indicate similar tendencies.

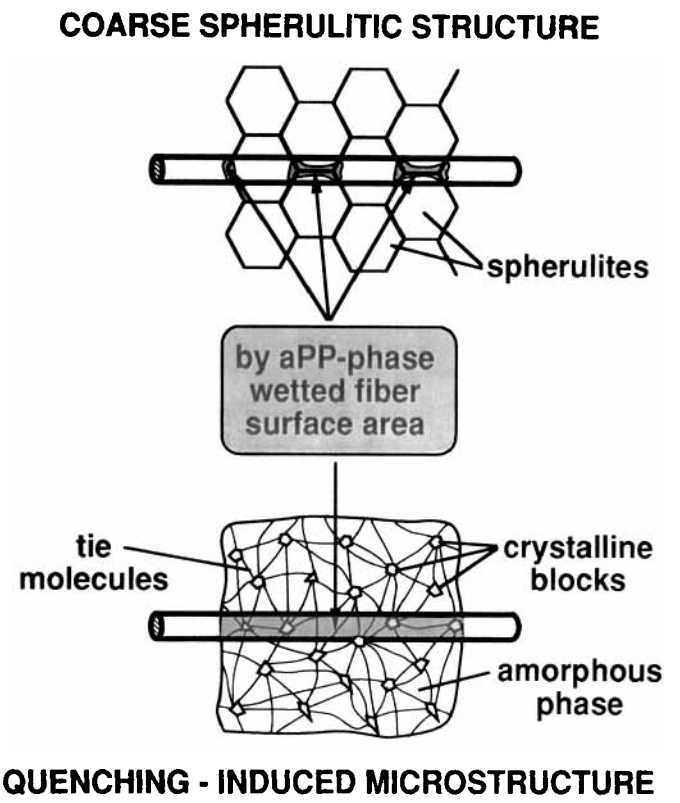

FIGURE 14 Schematic representation of the wetting behaviour of iPP as a function of the microstructure.

Interphase Modification

Results The interfacial shear strength values, τ_i, obtained from the microdroplet pulloff testing series on the GF/iPP-samples of varying interphase modification (fiber sizing and/or matrix coupling) are summarized in Figure 15 and Table II. Both mean values and the related standard deviations are listed for each material variation. In general, it is conspicious, as far as the combination "unsized fiber/uncoupled PP" is considered, that the τ_i-values gained from the modified pullout tests on isothermally-crystallized samples (4.8–5.8 MPa) correspond very well with those of the microdroplet pulloff tests (5.7 MPa). Therefore, both test methods provide absolutely comparable interfacial shear strength values. Furthermore, the PP-compatible aqueous sizing applied on the glass fiber surface increases τ_i substantially, *i.e.*, up to 17.1 MPa. Matrix coupling alone yields a similar value (17.7 MPa). Using both fiber sizing and matrix coupling results in a further improvement in interfacial shear strength (20.2 MPa).

The interphase failure seems to be controlled by shear stresses in the microdroplet pulloff test for all model composite variations. This is evidenced by the linear relationship between maximum debonding force F vs. embedded fiber length L (Figure 16).

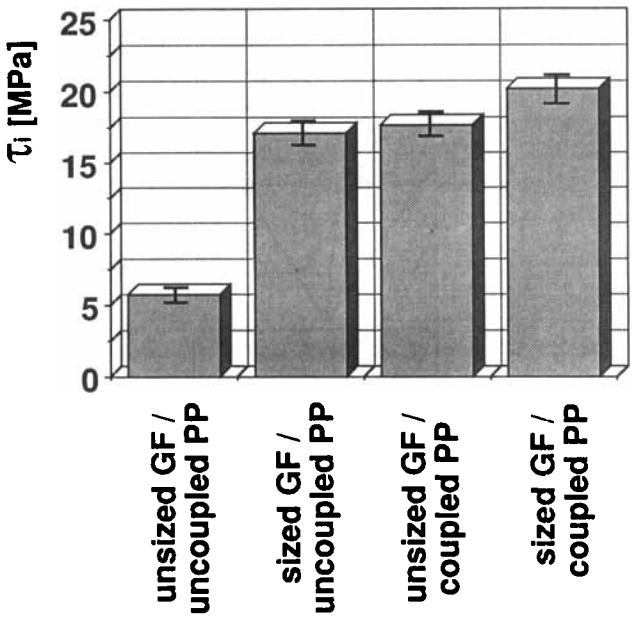

FIGURE 15 Comparison of interfacial shear strengths for GF/iPP of varying interphase modification (microdroplet pulloff test).

Discussion The fact that the interfacial shear strength in GF/iPP is much more affected by matrix coupling and fiber sizing than by the processing conditions clearly shows the strategies to be followed. Further investigations are, however, necessary in order to clarify the fine structure of the interphase[13] and its changes due to diffusion and segregation processes during the processing and service. A further open question is how the interphase parameters established in micro- or model composites can be used for prediction of the mechanical properties of real or macrocomposites. This topic was covered by a pioneering work of Drzal and Madhukar[35] performed on CF-reinforced epoxy composites. Unfortunately, an analogous work has not been devoted to semicrystalline thermoplastic matrix based composites.

TABLE II
Interfacial shear strength values for the microdroplet pulloff test

Fiber Surface Treatment	Matrix Modification	τ_i(mean) [MPa]	τ_i(st. dev.) [MPa]
unsized	uncoupled	5,7	1,0
sized	uncoupled	17,1	1,7
unsized	coupled	17,7	1,9
sized	coupled	20,2	1,9

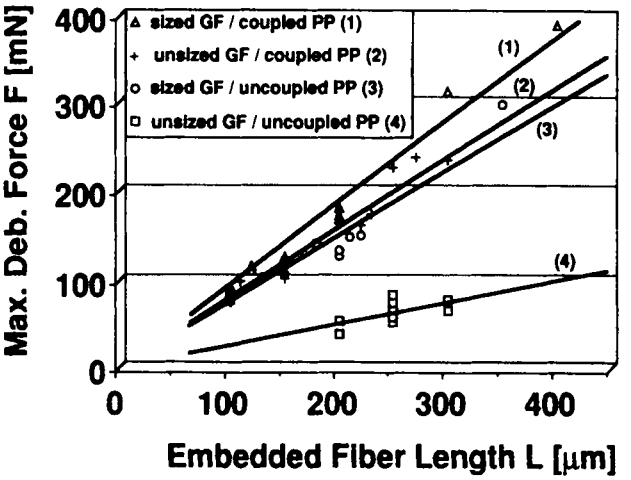

FIGURE 16 *F vs. L*-plots for GF/iPP of varying interphase modification (microdroplet pulloff test).

CONCLUSIONS

It was established by means of a modified single fiber pullout testing technique performed on GF/iPP samples of definite thermal prehistory that the adhesion, and thus the interfacial shear strength (τ_i), is not influenced by the matrix microstructure. Cooling-caused residual stresses and, thus, frictional effects do not enhance τ_i either. Increased interfacial shear strength for the quenched samples (from ≈ 5 to ≈ 9 MPa) was attributed to a better wetting and improved adhesion toward the GF given by the amorphous PP fraction formed. A schematic model considering the wetting behaviour of iPP and aPP was proposed. Based on this model, it was concluded that prerequisites of a high interfacial shear strength are good fiber wetting performance and high shear strength of the matrix. Since they are changing in the opposite direction in semicrystalline materials, an optimum between them should be targeted. This requirement can be met by using random PP copolymers of reduced crystallization ability. It was demonstrated for the GF/iPP model composites that the modified pullout and the microdroplet pulloff tests yield similar interfacial shear strength values. A further finding was that τ_i can be strongly increased by using proper fiber sizing or matrix coupling agents. Fiber sizing or matrix coupling alone yielded similar τ_i values (≈ 17 MPa). The combined use of fiber sizing and matrix coupling may have a synergistic effect on the interfacial shear strength (≈ 20 MPa).

Acknowledgement

The financial support of this work by the German Science Foundation (Interface Effects; DFG 675/13-1) is gratefully acknowledged. Part of this work was performed in a cooperative effort with the Department of Plastics and Rubber, TU Budapest, Hungary, sponsored by the Alexander-von-Humboldt Foundation.

References

1. E. Jenckel, E. Teege and W. Hinrichs, *Kolloid-Zeitschrift* **129**, 19 (1952).
2. A. J. Lovinger, J. O. Chua and C. C. Gryte, *J. Polym. Sci.* **15**, 641 (1977).
3. M. J. Folkes and W. K. Wong, *Polymer* **28**, 1309 (1987).
4. S. Incardona, C. Migliaresi, H. D. Wagner, A. H. Gilbert and G. Marom, *Composites Sci. Technol.* **47**, 43 (1993).
5. D. Rolel, E. Yavin, E. Wachtel and H. D. Wagner, *Composite Interfaces* **1**, 225 (1993).
6. C. Y. Yue and W. L. Cheung, *J. Mater. Sci.* **26**, 870 (1991).
7. H. Kobayashi, E. Hayakawa, T. Kikutani and A. Takaku, *Advanced Composite Mater.* **1**, 155 (1991).
8. H. D. Wagner, A. Lustiger, C. N. Marzinsky and R. R. Mueller, *Composites Sci. Technol.* **48**, 181 (1993).
9. A. Tregub, H. Harel and G. Marom, *Composites Sci. Technol.* **48**, 185 (1993).
10. S. Meretz, W. Auersch, C. Marotzke, E. Schulz and A. Hampe, *Composites Sci. Technol.* **48**, 285 (1993).
11. L. T. Drzal, "Optimum Design of the Fiber-Matrix Interphase in Composite Materials", in *Composites-ICCM/VIII* (15–19 July, 1991, Honolulu), S. W. Tsai and G. S. Springer, Eds., (SAMPE, Covina,CA, 1991), Paper 1-E.
12. L. T. Drzal and P. J. Herrera-Franco, "Composite Fiber-Matrix Bond Tests", in *Engineered Materials Handbook*, Vol. 3. (ASM International, Metals Park,OH, 1990), 391–405.
13. P. J. Herrera-Franco and L. T. Drzal, *Composites* **23**, 2 (1992).
14. F. J. Padden and H. D. Keith, *J. Appl. Phys.* **30**, 1479 (1959).
15. J. Varga, *J. Mater. Sci.* **27**, 2557 (1992).
16. E. Devaux and B. Chabert, *Polym. Communications* **31**, 391 (1990).
17. J. Varga and J. Karger-Kocsis, *Polym. Bulletin* **30**, 105 (1993).
18. J. M. Haudin, "Optical Studies of Polymer Morphology", in *Optical Properties of Polymers*, G. H. Meeten, Ed., (Elsevier Applied Science Publishers, London and New York, 1986), Chap. 4, pp. 167–264.
19. J. Varga and J. Karger-Kocsis, *Composites Sci. Technol.* **48**, 191 (1993).
20. J. L. Thomason and A. A. van Rooyen, *J. Mater. Sci.* **27**, 897 (1992).
21. B. S. Hsiao and E. J. H. Chen, "Transcrystalline Interphase in Advanced Polymer Composites", in *Controlled Interphases in Composite Materials*, H. Ishida, Ed., (Elsevier Science Publishing Co., New York, 1990), pp. 613–622.
22. J. L. Thomason and A. A. van Rooyen, *J. Mater. Sci.* **27**, 889 (1992).
23. B. P. Saville, "Polarized Light: Qualitative Microscopy", in *Applied Polymer Light Microscopy*, D. A. Hemsley, Ed., (Elsevier Applied Science, London, 1989), Chap. 4, pp. 111–149.
24. E. Devaux and B. Chabert, *Polym. Communications* **32**, 464 (1991).
25. P. C. Painter, M. Watzek and J. L. Koenig, *Polymer* **18**, 1169 (1977).
26. M. R. Piggott, "Interface Properties and Their Influence of Fiber-Reinforced Polymers", in *Composite Applications–The Role of Matrix, Fiber, and Interface*, T. L. Vigo and B. J. Kinzig, Eds., (VCH Publishers, New York, 1992), Chap. 9, pp. 221–265.
27. E. Mäder and K.-H. Freitag, *Composites* **21**, 397 (1990).
28. J. R. Dryden, *J. Mater. Sci. Lett.* **6**, 1129 (1987).
29. D. A. Biro, G. Pleizier and Y. Deslandes, *Composites Sci. Technol.* **46**, 293 (1993).
30. L. DiLandro, A. T. DiBenedetto and J. Groeger, *Polym. Composites* **9**, 209 (1988).
31. B. Z. Jang, "Fracture Performance in Continuous Fiber Reinforced PP", in *Polypropylene: Structure, Blends and Composites*, J. Karger-Kocsis, Ed., (Chapman and Hall, London, 1994), Chap. 3.9. (to appear).
32. W. A. Zisman, "Relation of the Equilibrium Contact Angle to Liquid and Solid Constitution", in *Contact Angle, Wettability and Adhesion*, R. F. Gould, Ed., (ACS, Washington, 1964), Advances in Chemistry Series Vol.43, pp. 1–51.
33. F. Hoecker and J. Karger-Kocsis, *Polym. Bulletin* **31**, 707 (1993).
34. L. Ye, A. Beehag and K. Friedrich, *Composites Sci. Technol.* (submitted).
35. L. T. Drzal and M. Madhukar, *J. Mater. Sci.* **28**, 569 (1993).